

PART VIII

DUST AND H II REGIONS

INTERFEROMETRIC STUDIES OF OH SOURCES ASSOCIATED WITH H II REGIONS AND IR OBJECTS

R. D. DAVIES

University of Manchester, Nuffield Radio Astronomy Laboratories, Jodrell Bank, U.K.

Abstract. An interferometer with a 24 km baseline has been used to map components of OH sources to a precision of a few hundredths of a second of arc. The W3 OH source which is associated with an H II region appears to be rotating slowly. There is evidence for Zeeman splitting in the components of this source. The IR/OH sources NML Cygnus and VY CMa are found to be expanding objects with a large rate of mass outflow. Rotation is also evident in both these objects.

1. Introduction

Interstellar OH is found in two main classes of object in the Galaxy. The first is the 'normal' interstellar cloud (or at least the more dense part of the distribution of these clouds) which probably contains the bulk of the molecules in the Galaxy. These clouds are sometimes observed in emission at radio frequencies but are most readily detected in absorption against background radio sources. The gas (hydrogen) density in these clouds is typically 10 to 10^3 hydrogen atoms cm^{-3} . The second class of OH object is the compact region which has a high brightness temperature in the spectral line as a result of masering action within the cloud. These objects have diameters of $\sim 10^{16}$ cm and gas densities estimated to lie in the range 10^8 to 10^{12} cm^{-3} . The present paper is concerned with new measurements of the second class of OH object.

The OH masering sources may themselves be subdivided into distinct groups each with its own properties. One group consists of the main line (1665 and 1667 MHz) emitters which are associated with H II regions; the satellite lines are weak. This group is strongly circularly polarized. Further, for a given source the velocities of the components in any one line are different from those of the other lines.

Another group contains those OH sources which are associated with IR sources; they are generally strongest in the 1612 MHz satellite line of OH. This group includes such diverse objects as the Mira variables, the Orion IR nebula, NML Cygnus and VY Canis Majoris.

Both the 'normal' and the masering clouds contain significant amounts of dust. The 'normal' clouds show a visual absorption ranging from a few tenths of a magnitude (Davies and Matthews, 1972) to 6–8 magnitudes (Heiles, 1968). The OH masering objects associated with H II regions have been found to be IR emitters in most cases (Wynn-Williams *et al.*, 1973). The IR emission from both groups of OH masering objects is believed to come from circumstellar dust clouds.

Interferometric studies of the spatial structure of the OH masering objects have been made at a number of observatories with baselines ranging up to several thousand kilometres. These have shown that the various emission components in the spectrum come

from separate regions with diameters typically a few hundredths or thousandths of a second of arc. The present observations have been taken with the 24 km baseline of the Mark II–Mark III interferometer at Jodrell Bank. They provide more definitive positions for the brighter OH masering sources than have been made so far.

2. The W3 OH Source

The W3 OH source lies at the edge of the H II region IC 1795. The OH source is within a few seconds of arc of a compact H II region visible only at centimetre wavelengths.

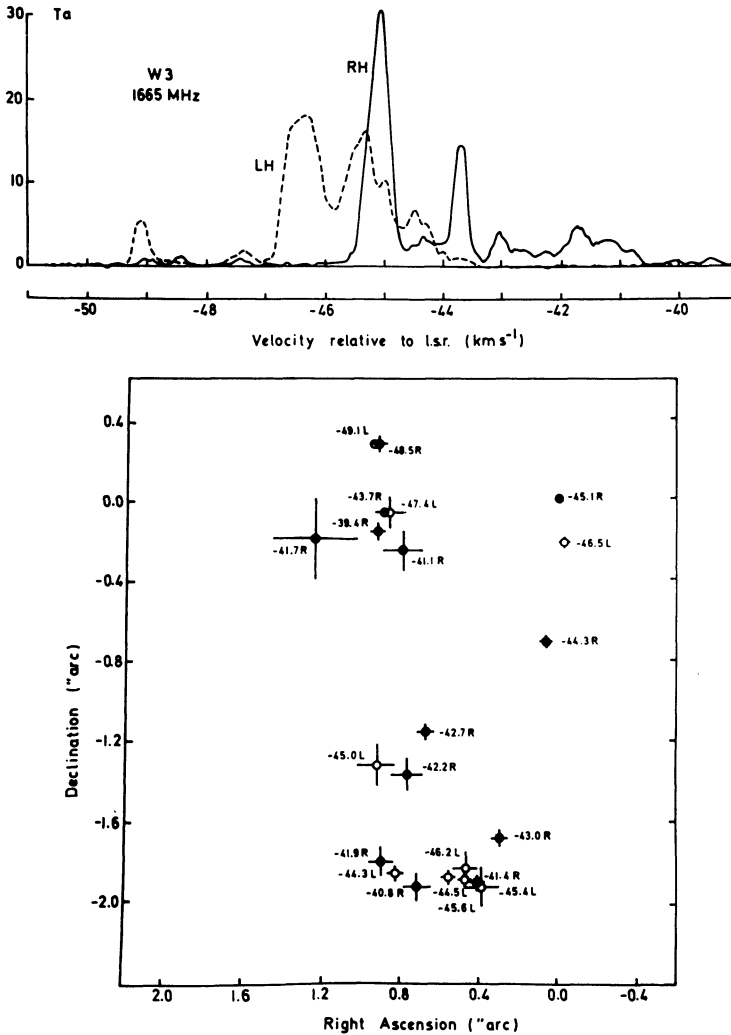


Fig. 1. The W3 OH source at 1665 MHz. LH and RH spectra taken with a single telescope are shown. The map gives the location of source components relative to the -45.1 km s^{-1} RH component.

An IR source has also been found within the position uncertainty of the OH source. (Wynn-Williams *et al.*, 1973). The OH source, H II region and IR object could be concentric.

The most detailed map of the 1665 MHz OH source published so far (Cooper *et al.*, 1971) was obtained with an observing baseline of 127 km s^{-1} . It showed that 13 components were scattered over a region $\sim 2''$ in diameter. Very long baseline interferometry (Moran *et al.*, 1968) has shown that the components have diameters ranging down to $0.0045''$.

New observations with the Mark II–Mark III interferometer have led to improved positions for 22 components. Although this number of components could not be conclusively identified in the RH and LH spectra alone, the interferometry provided the further means of separating the components in position as well as in frequency.

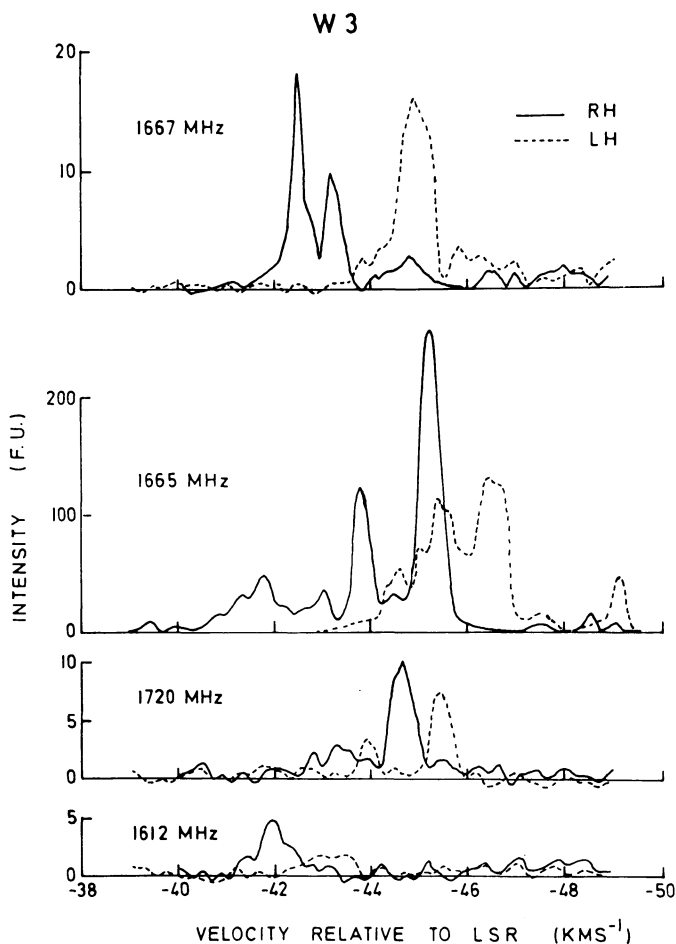


Fig. 2. W3 OH source spectra in the 4 lines of the ${}^2\Pi_{3/2}$, $J = \frac{3}{2}$ state showing displacement of the LH and RH polarization which is interpreted as the result of the Zeeman effect. The 1612, 1667 and 1720 MHz spectra are taken from Rydbeck *et al.* (1970).

Figure 1 shows the LH and RH spectra and the location of the components relative to the -45.1 km s^{-1} RH component obtained in the interferometry. The relative position accuracy ranges from $\sim 0.01''$ for the brighter components such as -49.1 km s^{-1} LH to $\sim 0.08''$ for the fainter components such as -45.0 km s^{-1} LH.

The components shown in Figure 1 probably represent the total number that exist in W3. They are spread over a region $2.5'' \times 1.4''$ with the major axis at p.a. = 174° .

At first sight the map of W3 does not show any clear pattern either in the distribution of velocity or polarization. Before examining this point further, attention will be drawn to another feature of the spectra of W3 which will help in the interpretation of Figure 1.

As soon as circular polarization was discovered in OH sources it was noticed that the LH and RH spectra of W3 were displaced relative to one another in the way which might arise from Zeeman splitting (Davies *et al.*, 1966). However when it was found that these sources were masering it became evident that the *simple* Zeeman pattern would not be preserved in the maser situation in different parts of the interstellar clouds. Nevertheless, on average, a relative displacement of the LH and RH spectra would be expected if a line-of-sight component of magnetic field existed in the OH cloud. In the case of W₃ this displacement in frequency of the LH and RH spectra has persisted as further ground and excited state transitions have been measured giving added weight to the Zeeman splitting interpretation. Figure 2 gives the LH and RH spectra of the 4 transitions in the $^2\Pi_{3/2}$, $J = \frac{3}{2}$ state. In each case the RH spectrum is displaced to positive velocity relative to the LH spectrum. An estimate of the longitudinal component of the field in each spectrum is given in Table I. In each case it has been derived from the displacement between the mean velocity of the LH and RH spectra. The theoretical Zeeman split for the 1612 and 1720 MHz lines was calculated as the mean displacement of the 3 theoretically expected components weighted by the component intensities. Table I suggests that the line-of-sight component of the magnetic field in W3 is $\sim 5 \times 10^{-3}$ G.

Figure 1 should give more explicit information about the validity of the Zeeman interpretation of the integrated spectra. It would be expected that the LH and RH components in the same or adjacent parts of the object should be displaced in the sense mentioned above. Indeed this is the case in every region of the map – the LH component is always displaced to lower velocities than the RH component. The mean

TABLE I
Magnetic fields in W3 derived from Zeeman interpretation

Line	Theoretical Zeeman split (MHz G ⁻¹)	Observed split (kHz)	Magnetic field (10 ⁻³ G)
1612 MHz	1.31	5.8	5.8
1665	3.27	14.1	4.3
1667	1.96	10.0	5.1
1720	1.31	4.6	3.5

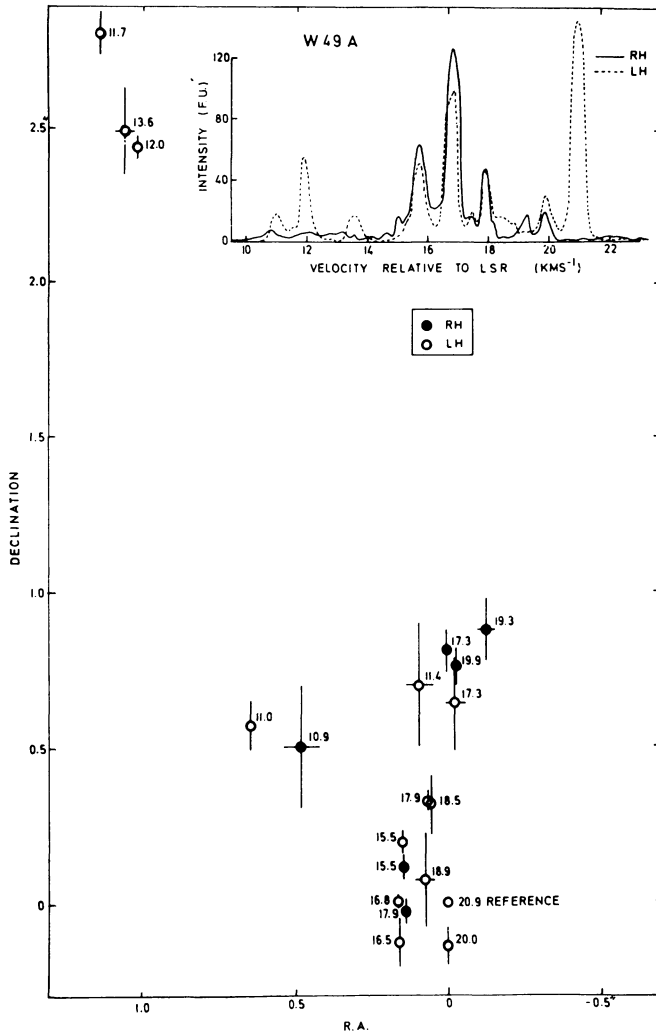


Fig. 3. The W49A OH source. This is the north preceding group of the W49 double OH source. The spectrum has been derived from the interferometric observations. Component positions in the map are plotted relative to the 20.9 km s⁻¹ LH component.

displacement within the various groups of features is 15.4 kHz; this corresponds to a magnetic field of 4.7×10^{-3} G directed away from the observer.

The further consequence of the Zeeman interpretation of the data is that local velocities can be calculated over the object. The velocity increases from the northern to the southern end of the object with a gradient of 1.5 km s⁻¹ per second of arc. This can most simply be interpreted as a rotation. The elongation of the W3 OH source is perpendicular to the inferred rotation axis, as would be expected for a flattened rotating object.

It is interesting to compare the magnetic field strength inferred from the present

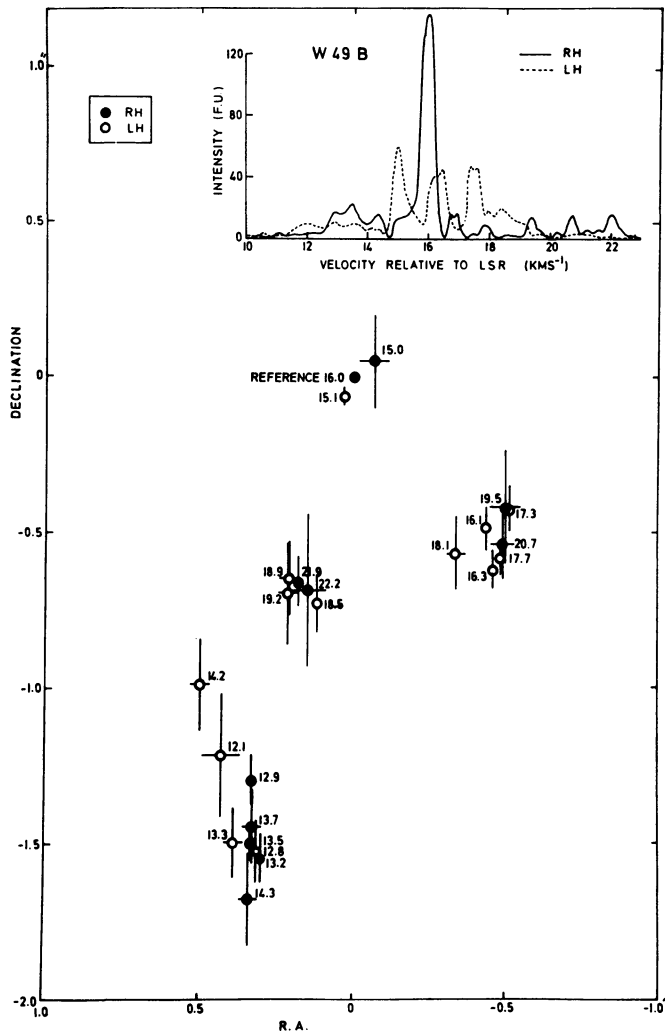


Fig. 4. The W49B source. The spectrum is derived from interferometer observations. Component positions on the map are plotted relative to the 16.0 km s^{-1} LH component.

measurements with that expected for a contracting interstellar cloud. We will take a field strength of $4 \times 10^{-6} \text{ G}$ to be typical of an interstellar cloud as determined from Zeeman effect measurements in neutral hydrogen absorption features. If a typical dimension of 10 pc is assumed then this field will be increased to $\sim 1 \text{ G}$ when the cloud contracts to a diameter of $2 \times 10^{-2} \text{ pc}$, the size of the W3 OH source. Clearly the original cloud has shed away most of its magnetic flux in contracting to the size of an OH masering cloud. Also it can be readily shown that the OH cloud must lose most of its magnetic flux in collapsing to form a star. It would therefore seem that the loss of magnetic flux is a continuing phenomenon in the condensation of interstellar clouds to form stars.

3. The W49 OH Sources (1665 MHz)

The W49 region contains two main groups of OH sources and associated H II regions. The north preceding OH group (W49A) lies 8.5 s of RA and 69.5" of Declination away from the south following OH group. Since the components of each group overlap in velocity it is only possible to separate the spectra of the two groups by interferometric observations. Figures 3 and 4 show the two spectra derived from the present observations.

The maps of the W49A and W49B OH sources are plotted in Figures 3 and 4; the position error in Declination is a factor of approximately 3 times the error in RA because of the low declination of these objects. W49A itself appears to consist of two groupings – one small group of LH components with velocities in the range 11.7 to 13.6 km s⁻¹ lies ~ 2.5" away from the main concentration.

W49B could be a cluster of 4 groups with diameters in the range 0.1 to 0.5". Such an interpretation is suggested by the small diameter/separation ratio, by the separation into velocity groupings and by the fact that there is no systematic velocity gradient across the whole region. These individual groupings would be similar in size to W3, which at the distance of W49 (14 kpc) would have an angular diameter of 0.3".

Of the 6 suggested groupings in W49 two show some evidence for the Zeeman splitting which was evident in W3. These are the groupings of W49B at the relative positions ($\Delta\alpha = +0.2''$, $\Delta\delta = -0.7''$) and ($\Delta\alpha = -0.4''$, $\Delta\delta = -0.5''$). The longitudinal component of magnetic field in these two groupings is 5×10^{-3} G directed away from the observer in each case. If the other groupings of components contain magnetic fields of this magnitude they must be highly inclined to the line of sight.

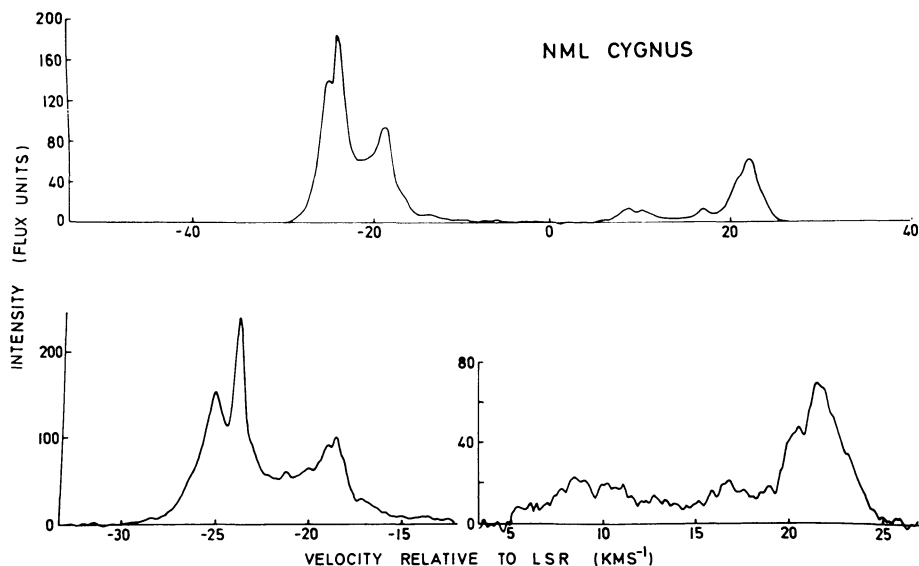


Fig. 5. The 1612 MHz spectrum of NML Cygnus. Top, a frequency resolution of 4.4 kHz. Bottom, a frequency resolution of 1.1 kHz.

4. The OH/Infrared Objects NML Cygnus and VY Canis Majoris

The infrared objects NML Cygnus and VY Canis Majoris have strong OH maser emission in the 1612 MHz line. They are associated with stars of M spectral type (M3e-M6) which are probably supergiants. A characteristic of their 1612 MHz spectra is the two peaks separated by $\sim 40 \text{ km s}^{-1}$. The redshifted peak is at the velocity of the M-star.

NML Cyg and VY CMA have similar spatial structures as determined by the interferometric observations. NML Cyg only will be described here in detail because it is a circumpolar source at Jodrell Bank and allows accurate relative positions to be determined. Its spectrum is shown at two frequency resolutions in Figure 5. A map of the main groups of components is shown in Figure 6.

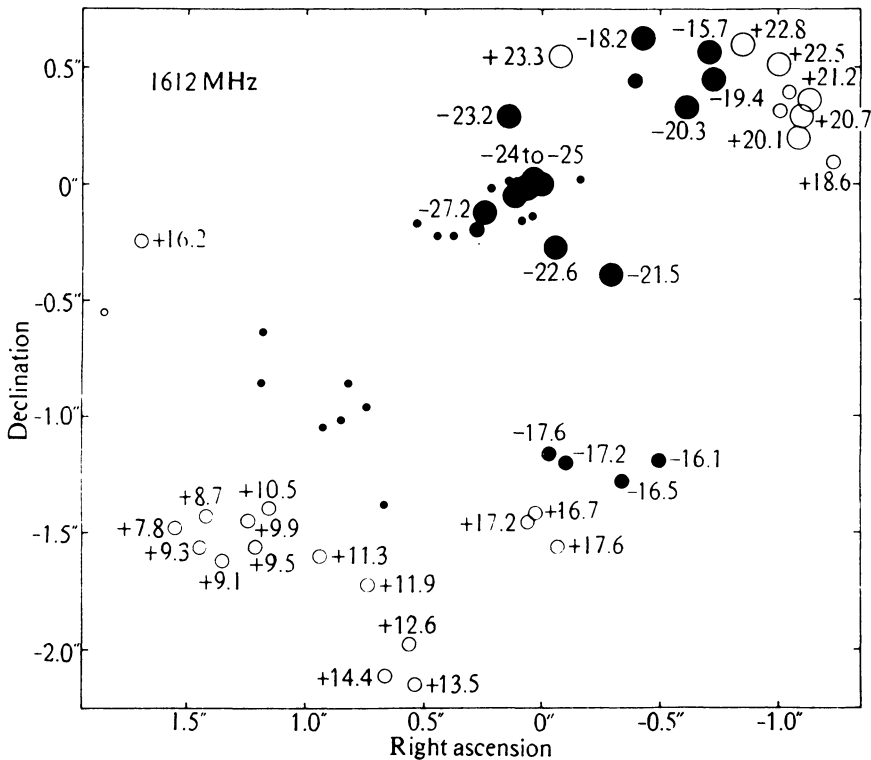


Fig. 6. A map of the principal features or groups of features in the 1612 MHz spectrum of NML Cygnus. The positive velocity end of the spectrum is plotted as \circ , and the negative velocity end as \bullet . The size of the symbols indicates the relative strength of the components.

The spatial structure of NML Cyg has a clearcut pattern; it is quite different from that found in the OH sources associated with H II regions such as W3 and W49. The components of NML Cyg lie in a region $3.3 \times 2.3''$ with its major axis at a position angle of 150° . The unique feature of the pattern in Figure 6 is that the components in

the positive (receding) velocity part of the spectrum lie outside those in the negative (approach) velocity part.

The observations plotted in Figure 6 can be understood in terms of the emission from an expanding gas cloud which is also rotating. The expansion accounts for the fact that the highest approach velocities occur at the centre of the object. Gas at the outermost edge of the object is expanding from the centre in a plane orthogonal to the line of sight; it is expected to have a radial velocity equal to that of the central star. The gas expanding away from the star on the far side of the object is not seen in the OH or H₂O lines. It is proposed that the molecular line radiation on the far side is obscured by a high density, partially ionized, central cloud. Figure 7 illustrates the present model of NML Cyg and VY CMa.

The physical parameters of these objects can be estimated on certain simplifying assumptions (Davies *et al.*, 1972). At a distance of 500 pc the diameter of NML Cyg is 2.4×10^{16} cm. The gas density within this diameter is 2×10^7 cm⁻³ leading to an estimated gas mass of $0.12 M_{\odot}$. If 10^{-3} to 10^{-4} of this gas is ionized it will be optically thick at the OH line frequency and obscure radiation from the far side of the object. The evidence of rotation comes from the observed gradient of the positive velocity gas; this gives a rotational velocity of 5 km s^{-1} at the outer edge which leads to a rotation period of 4200 yr. Another important parameter is the rate of mass outflow from the object. With the density and dimensions given above and an expansion velocity of 40 km s^{-1} , the rate of mass outflow is $3.5 \times 10^{-3} M_{\odot} \text{ yr}^{-1}$.

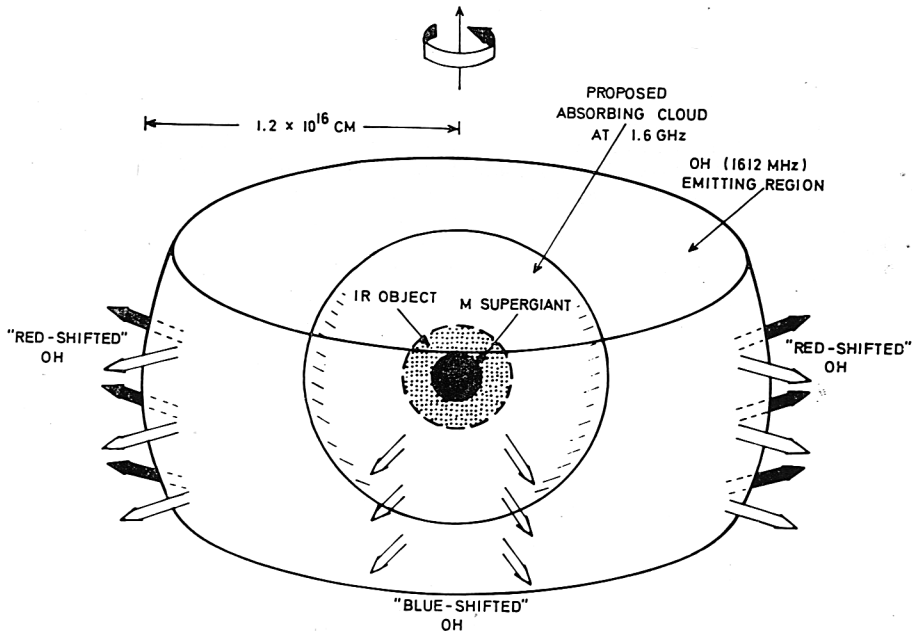


Fig. 7. The proposed model of NML Cygnus. The regions responsible for the redshifted and blue shifted features are indicated. The M supergiants has a radius of $\sim 2 \times 10^{14}$ cm and the IR object radius is $\sim 1.5 \times 10^{15}$ cm.

The above information provides substantial evidence that NML Cyg and VY CMa are in an early state of evolution. The cloud mass and rate of mass outflow is larger than has been found in any evolved star. It is most likely the remnant of the original cloud which condensed to form the M supergiant. Radiation pressure and thermal pressure from the absorbed stellar radiation are responsible for the present expansion of the gas and dust envelope. A further argument that these objects are remnants of the original cloud is their high angular momentum per unit mass – values far in excess of any evolved star.

The marked differences between the OH sources associated with infrared objects and those associated with H II regions are presumably attributable to the later stage of evolution of the gas cloud in objects like NML Cyg and VY CMa. In the H II region objects the gas cloud is presumably still contracting; it has a greater gas mass and a smaller velocity spread. In the 1612 MHz emitters the infall has been reversed to an outflow due to the action of the recently formed central star. In both stages large amounts of dust are present and become detectable in the infrared.

Acknowledgements

This paper describes work completed recently by the spectral line group at Jodrell Bank. Major contributions have been made by R. S. Booth, P. J. Harvey, M. R. W. Masheded, D. C. B. Whittet and A. Jane Wilson.

References

- Cooper, A. J., Davies, R. D., and Booth, R. S.: 1971, *Monthly Notices Roy. Astron. Soc.* **152**, 383.
 Davies, R. D., de Jager, G., and Verschuur, G. L.: 1966, *Nature* **209**, 974.
 Davies, R. D. and Matthews, H. E.: 1972, *Monthly Notices Roy. Astron. Soc.* **156**, 253.
 Davies, R. D., Masheded, M. R. W., and Booth, R. S., 1972, *Nature Phys. Sci.* **237**, 21.
 Heiles, C. E.: 1968, *Astrophys. J.* **151**, 919.
 Moran, J. M., Burke, B. F., Barrett, A. H., Rydbeck, O. E. H., Hansson, B., Rogers, A. E. E., Ball, J. E., and Cudaback, D. D.: 1968, *Astron. J.* **73**, S109.
 Rydbeck, O. E. H., Kollberg, E., and Elldér, J.: 1970, *Astrophys. J.* **161**, 125.
 Wynn-Williams, C. G., Becklin, E. E., and Neugebauer, G.: 1973, this volume, p. 459.